Parameters of Atmospheric Turbulence and the Dynamics of the Lower Ionosphere in Studies at the SURA Facility

N. V. Bakhmetieva[a], *, G. I. Grigoriev[a], G. R. Vinogradov[a], I. N. Zhemyakov[a],
E. E. Kalinina[a], and A. V. Pershin[a]

[a] Radiophysical Research Institute Lobachevsky State University, Nizhny Novgorod, Russia
*e-mail: nv_bakhm@nirfi.unn.ru

Abstract—The results are presented for studies of turbulent phenomena as a component of the lower ionospheric dynamics based on measurement of the characteristics of signals scattered by artificial periodic irregularities of ionospheric plasma. The experiments were carried out at the SURA heating facility (56.15° N; 46.11° E) in 2015−2019. The method is based on perturbance of the ionosphere with a powerful high-frequency radio emission and the creation of periodic plasma irregularities in the field of a standing wave, which forms upon the reflection from the ionosphere of a powerful radio wave radiated to the zenith; the irregularities are located with probe radio waves. New data on variations in the parameters of the lower ionosphere are obtained. The altitude profiles and time dependences of the velocity of turbulent and regular vertical motion of the medium, the temperature of the neutral component, and variations in the turbopause level are discussed. It is shown that turbulent motions, along with regular vertical transport, make a large contribution to the dynamics of the lower ionosphere. The velocity of the turbulent motion of the medium, at several m/s, is comparable in magnitude with the velocity of the regular vertical motion of the plasma and the neutral component. The turbopause level in the altitude interval 88−110 km is subjected to both fast and slow changes. The wave character of the turbopause level has been revealed.

1. INTRODUCTION

The region of the Earth's atmosphere at altitudes of 60−130 km, including the lower ionosphere, is characterized by extremely developed dynamics determined by variations in the temperature, density, electron concentration, horizontal and vertical motions, and the influence of underlying regions. Atmospheric waves propagate in this altitude region, and turbulent phenomena contribute to the mixing of air components, ensuring the constancy of the composition up to the turbopause altitude, at which turbulent mixing of the components is replaced by the diffusional separation of gases. Above the turbopause level, ambipolar diffusion begins to play a decisive role in the transport processes. The study of this region of the Earth's atmosphere, its inhomogeneous structure, and its dynamics is an urgent task in the study of the near-Earth space and the processes of radiowave propagation.

There are large number of publications on experimental and theoretical studies of the dynamics of the lower ionosphere. They reflect the results of experiments measuring various parameters of the neutral and ionized components of the atmosphere at these altitudes, as well as the results of the solution of a number of theoretical problems associated in many aspects with the interpretation of measurements of both regular and turbulent parameters of the medium. Various aspects of experimental and theoretical studies of the dynamics of the lower ionosphere are considered in the list of publications, which is far from complete: (Teptin and Stenin, 1977; Danilov et al., 1979; Hananyan, 1982, 1985; Kalgin and Danilov, 1993; Hocking, 1983a, b; 1996; Kirkwood 1996; Holdsworth et al., 2001; Hocking and Roettger, 2001; J. Fritts and Alexander, 2003; Pokhunkov et al., 2003; Offermann et al., 2006; Somsikov, 2011; Karpov and Kshevetsky, 2014; Perminov et al., 2014; Karpov et al., 2016; Vlasov and Kelley, 2014, 2015; Medvedeva and Ratovsky, 2017; Borchevkina and Karpov, 2018; Andreeva et al., 1991; Galedin et al., 1981; Kokin and Pakhomov, 1986; Schlegel et al., 1977).

The development of new methods and the technical support of measurements, the appearance of new instruments, and the permanently increasing role of digital methods to record data stimulate the study of dynamic phenomena in the lower ionosphere. This paper presents some new results of the study of atmospheric dynamics based on the application of a "heating" method, with disturbance of the ionosphere by powerful radio emission from the heating facility to determine many parameters of the medium. Thus, the goal of this work is to study the dynamics of the Earth's

lower ionosphere via the creation of artificial periodic irregularities (API) of the ionospheric plasma. It is based on the formation of irregularities during the reflection from the ionosphere of powerful high-frequency radio emission from the SURA heating facility (56.15° N; 46.11° E), their location with probe radio waves, and the measurement of the altitude-time characteristics of signals scattered by ionospheric plasma irregularities. Processes to determine many characteristics of the ionosphere and neutral atmosphere developed based on this method provide information on the electron concentration and the velocity of the vertical regular motion of plasma, the altitudinal-temporal variations in the temperature and density of the neutral component, the velocities of turbulent motions of the medium and the turbopause level, and some aeronomic parameters of the D region, and they make it possible to study the propagation of atmospheric waves in the lower ionosphere, the formation of sporadic ionization layers, and other natural phenomena. The paper mainly presents the results of experiments on the study of the dynamics of the lower ionosphere performed at the SURA facility in 2015–2019. If necessary, the results are used, and references are given to earlier publications on various aspects of the dynamics of the lower ionosphere.

2. METHOD FOR THE STUDY OF TURBULENT PHENOMENA IN THE LOWER IONOSPHERE BASED ON THE FORMATION OF ARTIFICIAL PERIODIC IRREGULARITIES

The study of ionospheric dynamics at altitudes of 60–120 km, including turbulent phenomena, was carried out via resonant scattering of radio waves by APIs of the ionospheric plasma. The theoretical outlines of the method, as well as methods developed on its basis to determine a large number of parameters of the lower ionosphere and neutral atmosphere, have been detailed in publications (Belikovich et al., 1999, 2006; Bakhmet'eva et al., 1996a, b; 2002; 2005; 2010a, b; Belikovich et al., 2002; Bakhmetieva et al., 2016a, b; 2017a, b; 2018). In these works and in the list of publications, the reader will find comprehensive information about our researches in this field; therefore, here, we will give very brief information about the measurement and research methods.

2.1. Formation and Relaxation of Inhomogeneities

The method used to study dynamic phenomena in the lower ionosphere is based on the formation of periodic irregularities when a powerful radio wave is reflected from the ionosphere with the formation of a quasi-periodic structure of the temperature and electron concentration due to uneven heating of the ionospheric plasma, as a result of which a periodic structure of temperature and electron density appears with spatial period Λ equal to half of the length λ of power-ful radio waves in the plasma (Belikovich et al., 1999; Belikovich et al., 2002; Kagan et al., 2002). During the sounding of aninhomogeneous structure with probe radio waves, they are scattered by plasma inhomogeneities. When the condition of backward Bragg scattering is observed, the receiving device receives a signal, the intensity of which is due to the in-phase summation of the waves scattered by each inhomogeneity.

The times of the development of inhomogeneities and their disappearance (relaxation) after the end of the heating are determined by the composition, density, and temperature of the atmosphere, the degree of dissociation and ionization and other ionospheric processes. In various ionospheric regions, different processes play a decisive role in the formation and relaxation of the APIs. For example, it is the temperature dependence of the coefficient of attachment (detachment) of electrons to neutral molecules in the D region; the diffusion redistribution of plasma under the action of excess pressure of the electron gas in the E region; and redistribution of the plasma under the influence of the striction force in the F region (Belikovich et al., 1999; Belikovich et al., 2002). The relaxation of inhomogeneities after the end of the heating in the E region occurs under the action of ambipolar diffusion and due to the temperature dependence of the coefficients of electron detachment from negative ions in the D region.

To locate periodic irregularities and record the signal scattered by them, pulsed radio sounding of the disturbed region with probe radio waves of the same frequency and polarization is used after the end of heatingfacility operation at the stage of the irregularity relaxation. The development of inhomogeneities can be studied during quasi-continuous heating of the ionosphere (Bakhmetieva et al., 2016b). The amplitude A and phase φ of the scattered signal are calculated based on digital recordings of the quadrature components of the scattered signal with an altitude step of 0.7–1.4 km and a temporal resolution of 15 s at each altitude. Their time dependences are then approximated by linear functions of the form $\ln A(t) = \ln A_0 - t/\tau$; $\varphi(t) = \varphi_0 + 4\pi V t/\lambda$. The relaxation time of the API (the relaxation time of the signal scattered by inhomogeneities) τ is determined from the decay of the signal amplitude by a factor of e. The velocity V of the vertical plasma motion, which at the altitudes of the lower ionosphere is equal to the velocity of the neutral component (Gershman, 1974), is determined from the phase φ change in time. Figures 1–3 show the initial measurement data, which are then used to determine the parameters of the ionosphere and neutral atmosphere.

Figure 1 shows the dependence of the scattered signal amplitude (brightness) on time (abscissa axis) and altitude (ordinate axis) during observations at 1200–1700 Moscow time on September 27, 2017. The signals scattered by inhomogeneities in the D region are seen at altitudes of 65–80 km; the signals scattered by the
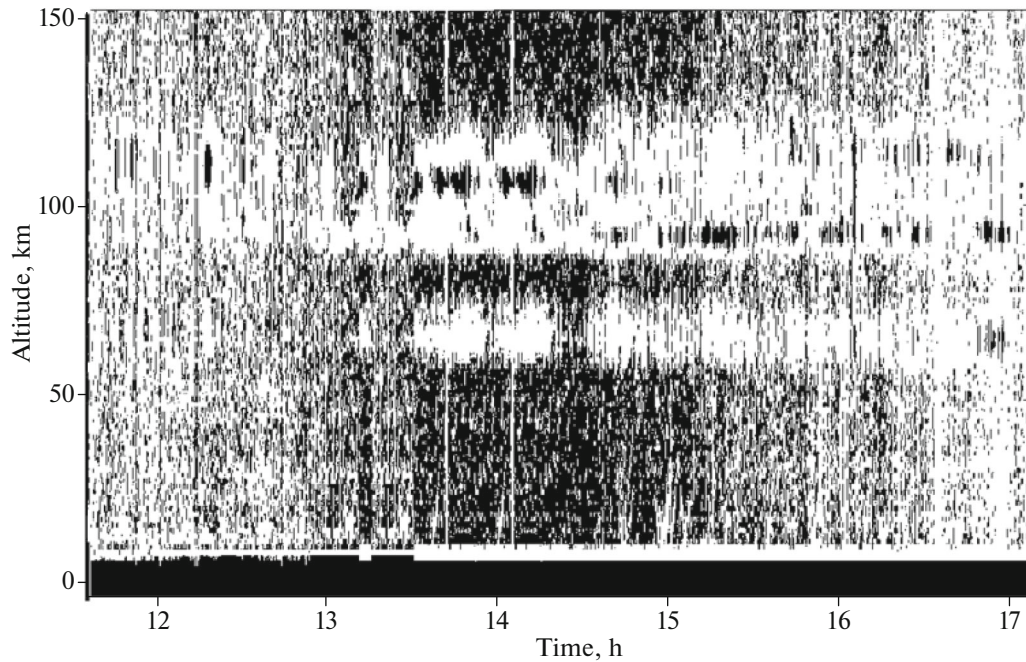
Fig. 1. Amplitude of the scattered signal in the coordinates: virtual altitude−time of observations on September 27, 2017. At altitudes of 65−80 km, the signals scattered by the API in the *D* region are seen; at altitudes of 90−130 km, the signals scattered by the API are seen in the *E* region.

API in the *E* region are seen at altitudes of 90−130 km. At an altitude of 90−95 km, a sporadic *E* (*Es*) layer appears as a thin reflection.

Figure 2 shows the dependence of amplitude (a) and relaxation time (b) of the scattered signal on time at three altitudes of 75.6, 99.4, and 110.8 km (the altitudes are shown from bottom to top) for observations on March 20, 2015. For convenience, the amplitude scale is shifted for each altitude by 50 dB, and the relaxation time scale is shifted by 5 s. Each point on the graphs corresponds to the amplitude and relaxation time averaged over 1 min (four measurements every 15 s). One can see an increase in the signal amplitude and a decrease, on average, in the relaxation time with increasing altitude. The scatter in the values of τ and their increase at certain time moments at 1200−1400 is due to the appearance of a sporadic *E* layer, which formed directly above the observation point at an altitude of 90−95 km and was recorded by an ionosonde.

The altitude profiles of the API amplitude and relaxation time are obtained during each 15-s recording of the scattered signal; typical examples are shown in Fig. 3. Each panel of Fig. 3 shows the altitude profiles of amplitude *A* (right curves) and relaxation time τ (left curves) measured at 1330 (Fig. 1a) and at 1445 (Fig. 1b) during observations on September 27, 2017, with averaging over a time interval of 15 min (curve with dots). Each altitude region of changes in the characteristics of the scattered signal is due to different ionospheric processes. For example, the law of relaxation under the influence of ambipolar diffusion corresponds to an altitude interval h of ∼95−130 km. The relaxation times in this range are in good agreement with the diffusion dependence τ(*h*). Below 95 km, atmospheric turbulence begins to affect, and the relaxation time of the scattered signal decreases in comparison with the characteristic diffusion time. At altitudes of 80−85 km, the amplitude of the scattered signal approaches the level of natural noise, and the change in the amplitude and relaxation time with altitude in the lower part of the *D* region is in complete accordance with the temperature dependence of the coefficient of electron detachment from negative ions (Belikovich et al., 1999; Belikovich et al., 2002).

The methods to determine many characteristics of the ionosphere and neutral atmosphere from the altitude dependence of the API relaxation time have been detailed (Belikovich et al., 1999; Belikovich et al., 2002; Tolmacheva et al., 2013, 2015; Bakhmetieva et al., 2018). Here, we will focus only on those that were used in this work.

2.2. Determination of the Temperature of the Neutral Component and the Velocity of Regular Vertical Plasma Motion

At altitudes without manifestation of the influence of atmospheric turbulence, the relaxation of inhomogeneities in the *E* region is due to ambipolar diffusion with a characteristic time
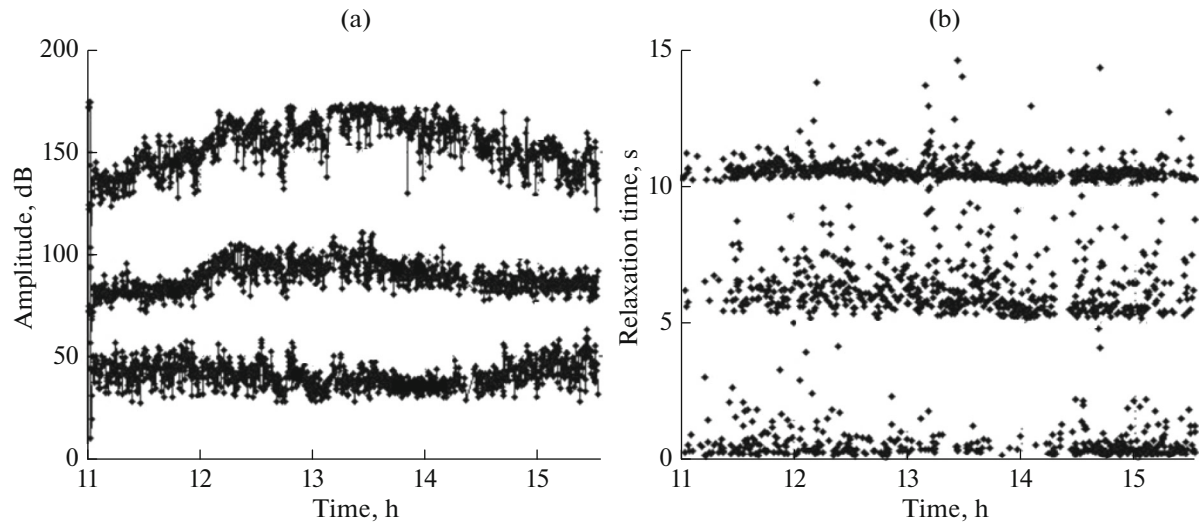
Fig. 2. Amplitude (a) and relaxation time (b) of the scattered signal at altitudes of 75.6, 99.4, and 110.8 km (from bottom to top) during observations on March 20, 2015. For convenience, the amplitude scale is shifted at each altitude by 50 dB, and the time scale is shifted by 5 s.

$$\tau = \frac{1}{K^2 D} = \frac{M_i \nu_{im}}{k_B(T_{e0} + T_{i0})K^2}, \quad (1)$$

where k_B is the Boltzmann constant; $K = 4\pi/\lambda$ is the wave number of standing wave; $\lambda = \lambda_0/n$ is the length of the powerful and probe radio waves in the medium; n is the refraction coefficient; D is the coefficient of ambipolar diffusion; M_i is molecular mass of ions; T_{e0} and T_{i0} are undisturbed electron and ion temperatures; and ν_{im} is the frequency of ion collision with neutral molecules. The methods to determine the electron concentration N, temperature T, and density ρ of the neutral component of the turbulent motion in the medium, the masses of dominating ions in the sporadic layer E (Es) are based on expression (1) (Belikovich et al., 1999; Bakhmetieva et al., 2005, 2010; Belikovich et al., 2002). In the absence of the Es layer and turbulence, the altitude dependence of the API relaxation time $\tau(h)$ corresponds to the diffusion approximation. Estimates have shown that the error in the temperature determination measurements with the API method does not exceed 10%.

The velocity of the vertical motion of the medium in the lower ionosphere is determined based on the fact that the plasma at altitudes of 50–120 km is a passive admixture and is carried away by the motion of the neutral gas. The velocity of regular vertical plasma motion V is directly determined from measurements of the phase of the scattered signal as

$$V = \frac{\lambda}{4\pi}\frac{d\varphi}{dt} = \frac{c}{4\pi fn}\frac{\Delta\varphi}{\Delta t}, \quad (2)$$

where λ and f are the length and frequency of the powerful and probe radio waves and n is the refraction index. Positive velocity values correspond to down-

ward motion. Belikovich et al. (1999, 2002) substantiated the estimate of the possible systematic error in the determination of V. Under normal ionospheric conditions, this error does not exceed $\Delta V \approx 0.05$ m/s for the extraordinary component of the probe wave, which we used to form and locate the API.

2.2. Determination of the Velocity of Turbulent Motion and the Turbopause Altitude

Even the first ionosphere experiments with the API method noted that the dependence of the relaxation time on the altitude of the E region does not correspond to the diffusion mechanism of inhomogeneity relaxation at all altitudes. It later became clear that this occurs in the region of the influence of turbulent diffusion. Figure 3 shows the influence of atmospheric turbulence on the relaxation time of the scattered signal. As seen from Fig. 3, the relaxation time first smoothly decreases with decreasing altitude and then, below a certain altitude, the decrease becomes more rapid. This occurs because inhomogeneities disappear (are destroyed) at altitudes below the turbopause level under the action of both ambipolar and turbulent diffusion. It is clear that the vortex motions caused by turbulence should affect the characteristics of the scattered signal, since they violate the ordered structure of inhomogeneities. They lead to dephasing of the signals scattered by different parts of the scattering volume, which naturally causes a decrease in the amplitude of the received signal and broadening of its angular spectrum. In this case, inhomogeneity relaxation occurs faster than under the action of ambipolar diffusion, and the relaxation time of the scattered signal decreases in comparison with the diffusion time. In the example shown in Fig. 3, atmospheric turbulence

begins to affect API relaxation below an altitude of 92−95 km. The relaxation times up to this altitude correspond to the diffusion dependence, but they become notably smaller than the diffusion values below the turbopause level h_t.

The potential to determine the turbulent velocity was theoretically considered in the literature (Belikovich and Benediktov, 1995; Belikovich et al., 1999; Belikovich et al., 2002), where the problem of the influence of the atmospheric turbulence on the amplitude and relaxation time of the API scattered signal has been solved in the approximation of the "frozen" velocity field of turbulent motions, distortion of the periodic structure only by the field of the vertical component of turbulent velocity (in the case of anisotropic turbulence), and some other assumptions. As a result, an expression was obtained for the amplitude of the signal scattered by the entire volume of inhomogeneities, which turned out to be dependent on the distribution density of the turbulent velocity V_t. Without dwelling on cumbersome mathematical calculations, we note that the simplest expression for the amplitude of the scattered signal is obtained if we assume the Cauchy distribution:

$$A(t) = A_0(1 + \tau_d/\tau_t)^{-1} \exp[-(1/\tau_d + \sqrt{2}/\tau_t)t], \quad (3)$$

where, τ_d is the time of diffusion, and τ_t is the time due to turbulent diffusion. In this expression for the amplitude of the scattered signal, its relaxation time τ, which is determined from the decrease in the measured amplitude signal by a factor of e, is described by formula $\tau^{-1} = (\tau_d^{-1} + \sqrt{2}\tau_t^{-1})$, and the turbulent velocity is given by the expression

$$V_t = (K\tau_t)^{-1} = (\tau^{-1} - \tau_d^{-1})/\sqrt{2}K. \quad (4)$$

In this case, the measured relaxation time above the turbopause level is determined by ambipolar diffusion.

Figure 4 explains further steps to find the value of V_t from the altitudinal dependence of the relaxation time of the scattered signal. The diffusion dependence $\tau_d(h)$ found from measurements of the amplitude above the turbopause level is extrapolated to lower altitudes $h < h_t$. As a result, the altitude dependence of the diffusion relaxation time $\tau_d(h)$ below the turbopause level is found, and the value of τ_d at each altitude is determined; the value of τ is determined from the results of a decrease in the measured amplitude by a factor of e, and the value of the turbulent velocity V_t is found from formula (4) (Belikovich and Benediktov, 1995; Bakhmet'eva et al., 1996a; Belikovich et al., 1999; Belikovich et al., 2002; Bakhmetieva et al., 2018).

In order to eliminate the error in the determination of the turbulent velocity due to extrapolation of the altitude profile of the relaxation time to the altitudes below the turbopause level, the experiment uses the method of API formation at two different frequencies, i.e., with different spatial scales (Belikovich et al.,
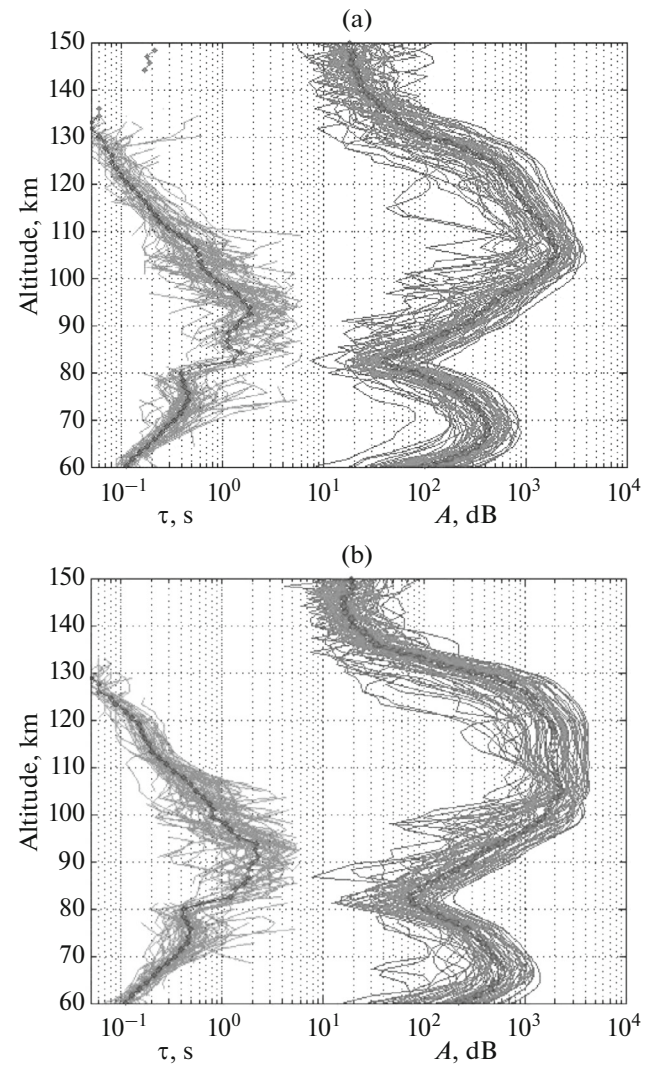

Fig. 3. Altitude profiles of amplitude A (right curves) on each panel and relaxation time τ (left curves) at each minute in sessions 1330−1345 (a) and 1445−1500 (b) during observations on September 27, 2017. Black curves with dots correspond to the averaged profiles A and τ over a time interval of 15 min.

2006; Bakhmet'eva et al., 2008). With this method, the electron concentration is determined from the ratio of the inhomogeneityrelaxation times at two frequencies, and the turbulent velocity and the ambipolar diffusion coefficient can be found independently of each other, as a result of which there is no need to extrapolate the $\tau_d(h)$ dependence to altitudes below the turbopause level (Bakhmetieva et al., 2018). In this case, inhomogeneities are formed alternately at two different frequencies f_1 and f_2, and the relaxation times of the scattered signal τ_1 and τ_2 are determined for each of the frequencies. The error in the determination of the turbulent velocity with this method does not exceed a few cm/s.
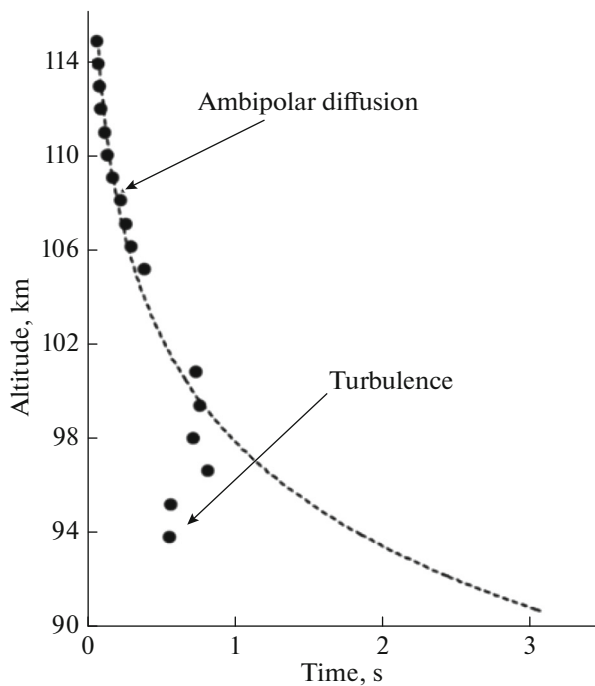
Fig. 4. Altitude dependence of the scattered signal amplitude on October 6, 2016: an example of the influence of atmospheric turbulence. The dotted line shows the dependence of the amplitude on the altitude in the case of the influence of ambipolar diffusion on the amplitude of the scattered signal at the API relaxation stage.

It is also clear from Fig. 4 where the turbopause level is located. Without going into detail on the discussion of different definitions of the turbopause altitude (Lehmacher et al., 2011; Offerman et al., 2006; Tolmacheva et al., 2019), we note that there is every reason to consider the turbopause altitude location at level h_t, below which turbulent diffusion begins to affect the relaxation time of the signal scattered by artificial periodic irregularities. This was confirmed in long-term experiments on the ionosphere with the API method. In the examples shown in Fig. 3 and Fig. 4, the effect of turbulence begins below 90−100 km and, obviously, the turbopause level is close to this altitude.

3. RESULTS OF THE DETERMINATION OF TURBULENCE PARAMETERS

The paper presents the results of the processing of a large array of measurement data of the amplitudes of signals scattered by inhomogeneities and presents the results of the determination of the velocity of turbulent motion of the medium at altitudes below the turbopause level. For the selected sessions of amplitude measurements, the altitude dependence of the relaxation time was relatively smooth and did not contain signs of the influence of the sporadic E layer, which is expressed by a local increase in the relaxation time at the altitudes of the Es layer (Bakhmet'eva et al., 2005,

2010a). The time period of study was from 2015 to 2019. Due to technical reasons, the experiments were carried out mainly in the autumn−summer period. To determine the magnitude of the turbulent velocity, we used the results of measurements of the amplitude of the signal scattered by the API in 2015 (August 12 and 13), 2016 (September 27 and 30), 2017 (August 9, September 26 and 28), 2018 (from September 25 to 28), and 2019 (September 11).

3.1. Turbulent Velocity

The experimentally determined relaxation time τ at each altitude was found from the altitude profile of the scattered signal amplitude, and the diffusion time τ_d was found from the curve of extrapolation of the diffusion dependence to the altitudes below the turbopause level. The turbulent velocity V_t was then calculated with formula (4). Figure 5 shows examples of the V_t velocity profiles obtained with this method for experiments carried out in August−September in different years. Here, the values of the turbulent velocity were calculated from the values of the relaxation time averaged over every 2 min. A common feature in the altitude profiles is an increase in turbulent velocity with a decrease in altitude from almost zero values at the turbopause level to several m/s at altitudes of 80−86 km, i.e., in fact, at the altitudes of the mesopause. Along with smooth V_t profiles, profiles that have a two-stage or irregular character of velocity variation with altitude are always observed.

The results of the determination of the turbulent velocity for three days of observations are accumulated in Fig. 6 in the form of a "cloud of dots," namely, from 1800 to 1900 Moscow time on August 12, 2015, from 1700 to 1800 on September 28, 2017, and from 1245 to 1545 on September 28, 2018. As a rule, each point on the graphs was obtained via averaging of the relaxation time of the scattered signal over a time interval of 5 min.

Let us focus on some features of the altitudinal-temporal variations of the turbulent velocity. First, the variability of the speed over time is manifested in Fig. 6 as a scatter of its values at each altitude. The maximum scatter was of the order of $\Delta V_t = 5$ m/s at an altitude of 95 km during observations on August 12, 2015. The maximum value of the velocity at this altitude was 6 m/s. In the observations of September 28, 2017, and September 28, 2018, the maximum ΔV_t scatter ranged from 1.5 m/s to 2.2 m/s at altitudes of 90−93 km. The maximum values of turbulent velocity $V_t = 2.2−4.5$ m/s were obtained at altitudes of 82−85 km, i.e., at the altitudes of the mesopause. Second, wavelike changes in the turbulent velocity with altitude with a period (scale) of several km were observed in many sessions. Third, the turbulent velocity is comparable in magnitude with the velocity of the vertical regular motion of plasma, which is equal to the velocity of the neutral component. Fourth, the turbulent velocity increased
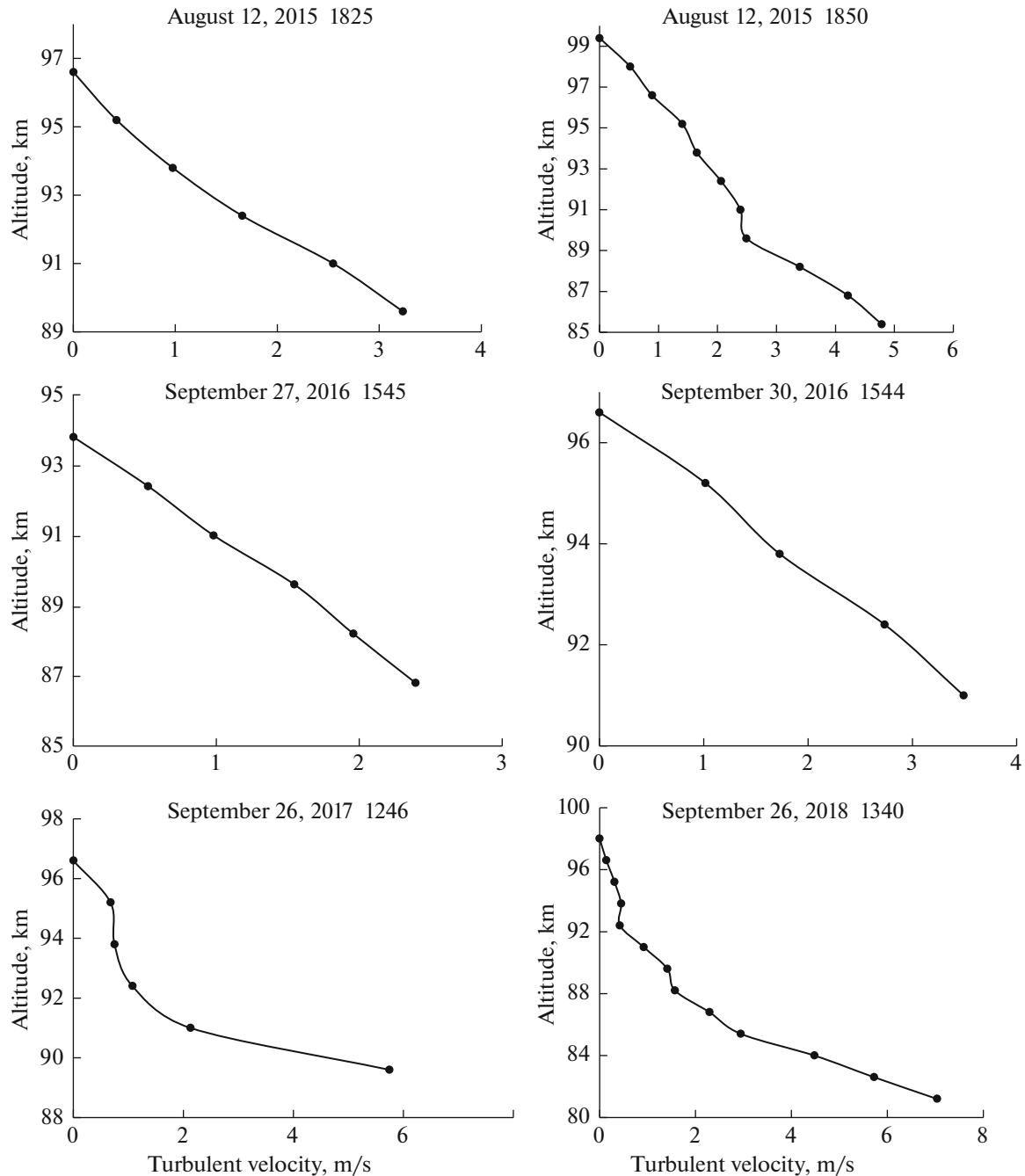
Fig. 5. Typical altitude profiles of the turbulent velocity obtained from the relaxation time averaged over 2 min during individual observation sessions. Both relatively smooth dependences $V_t(h)$ with a smooth increase in velocity with distancing altitude from the turbopause level and profiles with an irregular change in $V_t(h)$ are presented.

to 10−15 m/s in some cases at the lower boundary of the investigated interval. These V_t values seem to be unrealistic, and the reason for their appearance has not yet been revealed. They were excluded from the analysis and are not presented on the graphs. For comparison, we note that Holdsworth et al. (2001) obtained turbulent velocities of up to 6 m/s at an altitude of 95 km from measurements of the Buckland

Park MF radar (mid frequency radar of the partial reflection installation). In general, the determination of the turbulentmotion velocity from measurements of the characteristics of signals scattered by artificial periodic inhomogeneities showed that turbulent motions, along with regular vertical transport, make a large contribution to the dynamics of the lower ionosphere and should be taken into account in the mea-
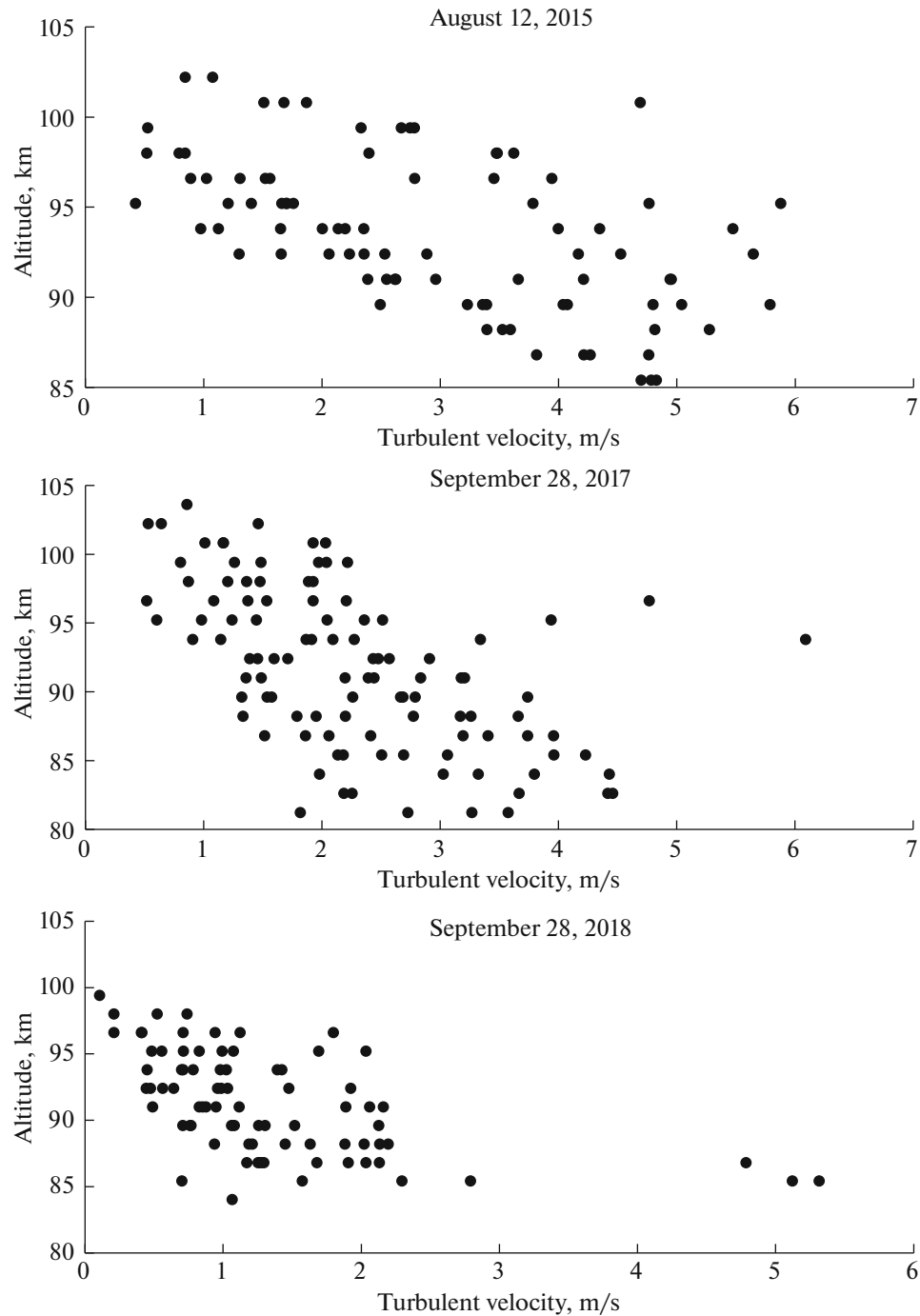
Fig. 6. Dependences of turbulent velocities on altitude ("clouds of dots") plotted for three days of observations on August 12, 2015, September 28, 2017, and September 28, 2018 at altitudes below the turbopause level.

surement of the parameters of the neutral component in this altitude range.

3.2. Altitude of the Turbopause

The decrease in the amplitude of the scattered signal under the influence of the atmospheric turbulence begins at the turbopause level. Tolmacheva et al.

(2015) presented and discussed the first results of the determination of the turbopause level based on the study of the ionosphere with the API formation method in 2007−2014. A detailed analysis of the altitude profiles of the relaxation time obtained in these experiments showed that the minimum possible altitude to determine the parameters of the neutral atmosphere (temperature and density) with this method

can be considered a marker of the turbopause level. According to the observational data given by Tolmacheva et al. (2015), it was concluded that the average level of the turbopause was 99−102 km in the autumn season. In the evening hours, this border tended to decrease to 94 km. The turbopause level generally varied in an altitude range of 94−106 km. Its variations often had a wavelike component with periods from 10−15 to 30−40 min. It was also concluded that the region with turbulence can increase to 110 km under conditions of developed convective instability, with a significant increase in temperature.

These conclusions are generally confirmed by the results of new experiments performed at the SURA facility in 2015−2019. Figure 7 shows examples of time variations in the turbopause level h_t based on observations in the daytime hours of October 27, 2018, October 26, 2018, and October 28, 2017. Each dot in Fig. 7 corresponds to averaging of the relaxation time over 5 min. Data on other days of observations in the specified time period were given earlier (Bakhmet'eva et al., 2020; Bakhmetieva et al., 2019). It generally follows from the results that the turbopause level h_t can vary in a fairly wide range of altitudes from 88 to 110 km. This means that the minimum turbopause level can decrease to altitudes close to the mesopause. Returning to Fig. 6, we note that the turbopause level in the previous examples was in the altitude interval 95−103 km on August 12, 2015, in the interval 97−103 km on September 28, 2017, and in the 97−100 km interval on September 28, 2018.

Data on the turbopause altitude presented by Hall et al. (2016) based on observations with a meteor radar at a latitude of 52° N indicate that this altitude varied from 95 to 107 km during the year, with an increase in individual values to 110 km.

The variability in the turbopause level over time and the wavelike nature of variations is a common feature in the turbopause level on these and other days. The dashed line in Fig. 7 shows a polynomial trend of the sixth order (approximation of the temporal dependence by a polynomial of the sixth degree, which is most suitable for the given conditions). Along with comparatively fast variations with a period of 5−15 min, longer variations are noted: from 30 min to several hours. However, we note that the nature of the change in the turbopause level of in time is different under conditions that are similar in geomagnetic and solar activity on days close to the autumn equinox. In this relation, the example of October 28, 2017, is especially interesting, which shows that the turbopause level experiences oscillations that increase in amplitude with a predominant period of 25−30 min. These fluctuations are superimposed on the faster h_t variations. Similar fluctuations in the turbopause level were also observed on October 27, 2017 (Fig. 11b in Bakhmetieva et al., 2020). The present results, together with the results of Tolmacheva et al. (2015) and Bakhmetyeva et al.

(2020), indicate that such wavelike variations in the turbopause level are caused by the propagation of internal gravity waves (IGWs) through the mesosphere and lower thermosphere. In addition, Tolmacheva et al. (2013) analyzed the effect of convective instability on variations in the turbopause level, and it was noted that an increase in h_t to an altitude of 110 km was observed during a significant increase in the temperature of the neutral component.

4. VARIATIONS IN TEMPERATURE AND VERTICAL VELOCITY

Vertical motions in the lower ionosphere are one of the main components of atmospheric dynamics. Measurement of the phase of the signal scattered by irregularities allows direct measurements of the vertical transfer rate. Digital recording of the scattered signal quadrature components allows the recording of fast fluctuations of the vertical velocity. The results of measurements of the rate of vertical transport with the API method in different years under different ionospheric conditions and natural phenomena were presented in the literature (Belikovich et al., 1999; Belikovich et al., 2002; Bakhmet'eva et al., 1996b, 2010a, 2016, 2017). The monthly average values of the velocity were ~1 m/s at altitudes below 100 km and increased to 5 m/s with an increase in altitude. It should be noted that the existing models of the circulation of the middle atmosphere at altitudes of 80−100 km result in average values of the velocities of vertical motions of only up to several cm/s (Izmereniye ..., 1978; Karimov, 1983). The vertical motions in the lower ionosphere are characterized by rapid time variations in the magnitude and direction of the velocity within 15 s, i.e., during one measurement. The velocities at certain time moments can be as high as 10 m/s or more during one measurement, and the velocities averaged over a 5-min time interval, as a rule, vary from −5 to +5 m/s. As a result of many years of research, the authors of this work concluded that relatively large vertical velocities are caused by wave motions in the atmosphere. As shown by Belikovich et al. (1999), IGWs can contribute to variations in the vertical velocity up to 10−12 m/s. During the analysis of the temporal dependence of the vertical velocity, wave motions with a period from 5−10 min to 4−5 h were found. The period (scale) of waves over altitude was 5−25 km (Bakhmet'eva et al., 1996b, 2010a, 2016, 2017; Belikovich et al., 1999; Belikovich et al., 2002; Bakhmetieva et al., 2018). The periods of the waves contributing to the velocity variations correspond to the periods of IGWs (Hines, 1975; Karimov, 1983; Brunelli and Namgaladze, 1988; Grigoriev, 1999; Fritts and Alexander 2003; Somsikov, 2011; Karpov et al., 2016; Borchevkina and Karpov, 2018).

To study the relationship between the temperature variations of the neutral component T and the velocity of regular vertical motion of the medium V at altitudes of 85−120 km, both parameters were determined
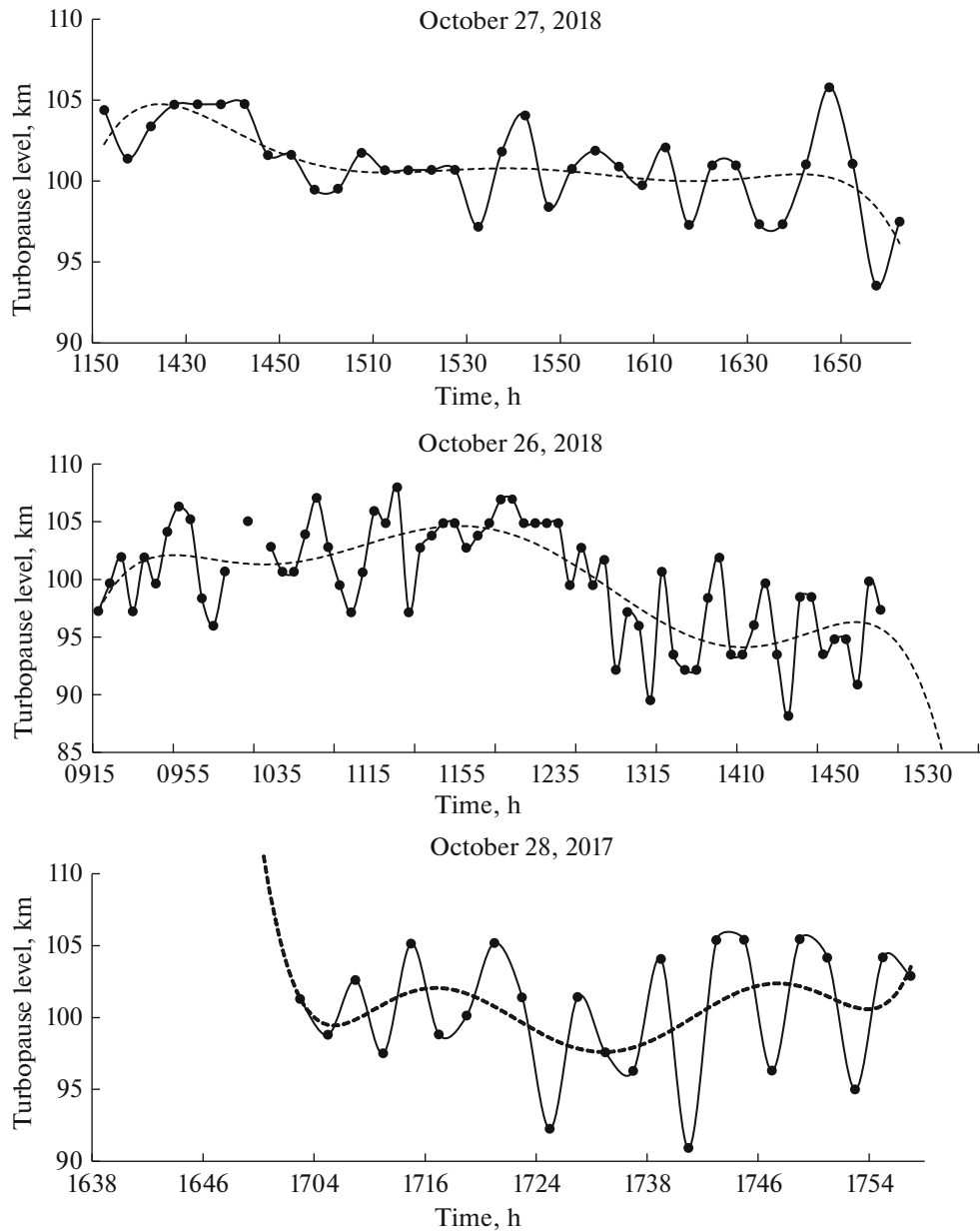
Fig. 7. Variations in time of the turbopause level for three days of observations on October 27, 2017, October 28, 2017, and October 26, 2018. Each point on the graphs was obtained from the relaxation time values averaged over 5-min intervals at each altitude. The dotted line shows the 6-h order polynomial trend (approximation of the time dependence with the 6-h order polynomial, which is most suitable under the given conditions).

simultaneously from measurements of the amplitude and phase of the signal scattered by inhomogeneities. Note that this problem was considered, in particular, by Tolmacheva et al. (2013) based on temperature and velocity measurements in experiments in September 2010 and September–October 2014. As a result, the following main features were identified in a comparison of the altitude profiles of the temperature T and velocity V: (*a*) a local temperature maximum was observed at the same altitude as the maximum of the absolute value of velocity, or, on the contrary, a mini-

mum of the absolute value of velocity was noted at the altitude of the local temperature maximum; (*b*) in the presence of a superadiabatic temperature gradient, convective instability was observed above the turbopause level; (*c*) undulating changes were almost always found in the altitude profiles of T and V.

The results of the determination of the neutral-component temperature in different ionospheric conditions were given in the literature (Belikovich et al., 1999; Bakhmetieva et al., 2010b, 2020; Tolmacheva et al., 2013; Bakhmetieva et al., 2013, 2019; Tolmacheva
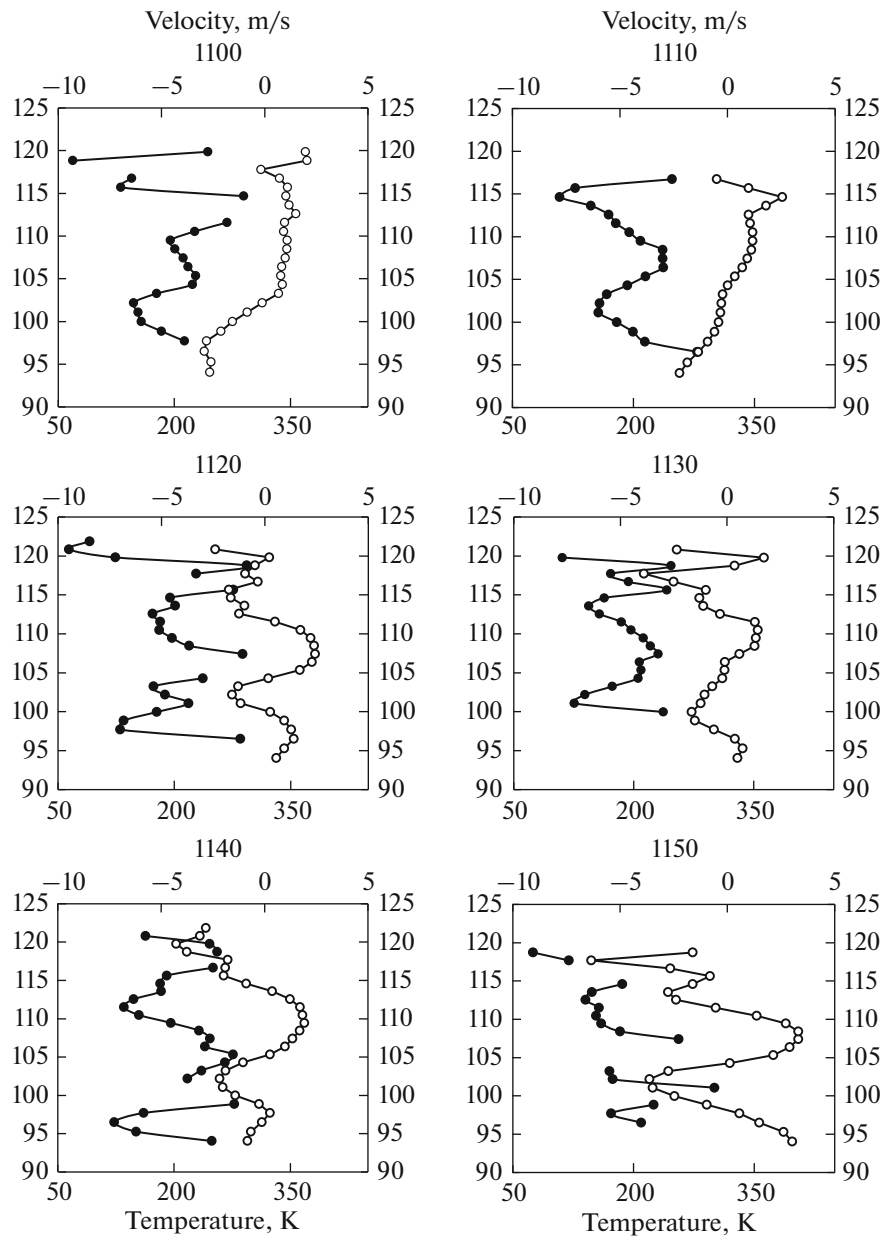
Fig. 8. Altitude profiles of the temperature of the neutral component (points, lower scale) and the velocity of vertical motion (circles, upper scale) during six consecutive sessions from 1100 to 1200 (observations on October 25, 2018). Each graph was obtained via averaging of the data over a 10-min interval.

et al., 2013, 2015). In this paper, we supplement these results with new information. Figure 8 shows the altitude profiles of the neutral-component temperature and the velocity of the vertical motion of medium during six successive sessions of observations from 1100 to 1200 on October 25, 2018. Each graph was obtained via averaging of the temperature and velocity values over a 10-min interval with a step in altitude of 1.4 km. With a few exceptions, the temperature in the altitude interval 90–120 km varied from 100 to 250 K. It sometimes dropped to 50 K, which is not confirmed by the results of measurements by other methods and

has not yet found an explanation. Figure 8 shows irregular altitude variations in the temperature and undulating variations in vertical velocity. Positive speed values are related to downward motion. The predominant scale (period) in altitude was 5–15 km. The velocity changes sign with altitude almost on all panels of Fig. 8 at an altitude of ~105 km; hence, the direction changes from upward motion of the medium to downward motion. There are two important points to note. First, when the velocity changes sign as it crosses the zero value such that ascending motions are replaced by descending ones (this takes place at an altitude of 102–
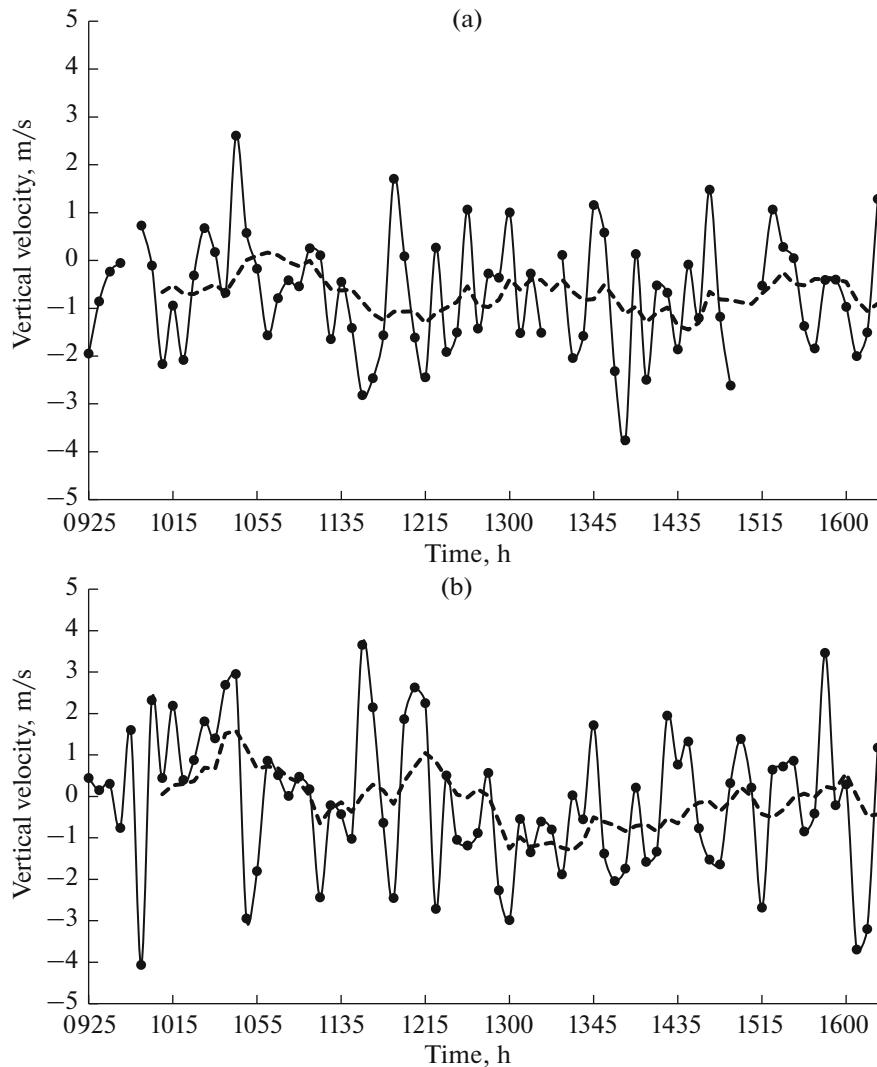
Fig. 9. Temporal dependence of the velocity of vertical motion at an altitude of 100 km (a) and 105 km (b) during observations on October 25, 2018. Each point on the graphs was obtained via averaging of the velocity values over 5 min. The dashed curve was obtained with the running-average method over an interval of 40 min (8 points) in order to smooth out fluctuations of smaller periods.

105 km in almost every panel of the given figure), conditions are formed for redistribution of positive metal ions and, accordingly, the redistribution of electrons in an inhomogeneous velocity field and the formation of a sporadic E layer (Es). According to the results of observations, this altitude (the transition of the velocity through the zero value) corresponds, as a rule, to the altitude of the maximum of sporadic E layer. This indicates that the Es layer forms directly above the observation point as a result of the redistribution of charged particles in the Earth's magnetic field according to the theory of wind shear (Axford and Cunnold, 1996; Gershman, 1974; Gershman et al., 1976; Whitehead, 1961; Mathews, 1998). The existence of the sporadic E layer is confirmed by data from the CADI ionosonde located at the observation point near the SURA facility and is also clearly seen in the records of

the scattered signal amplitude, which is similar to that shown in Fig. 1. The Es layer causes the appearance of local maxima on the altitude profiles of the amplitude due to an increase in the electron concentration and relaxation time caused by the proportionality of the latter to the mass of ions, which in the sporadic E layer are represented by positive ions, often heavy ions of iron and calcium (Bakhmet'eva et al., 2005, 2010a). Second, the question of the probable correlation of the temperature and vertical velocity at the same altitude turned out to be difficult to interpret, which was partially considered by Tolmacheva et al. (2013). For example, Fig. 8 shows that the temperature and velocity change "in phase" in the altitude interval 100−120 km in sessions starting at 1120 and partially at 1130, i.e., the temperature maximum is reached at the same altitude as the maximum of the absolute value of velocity,
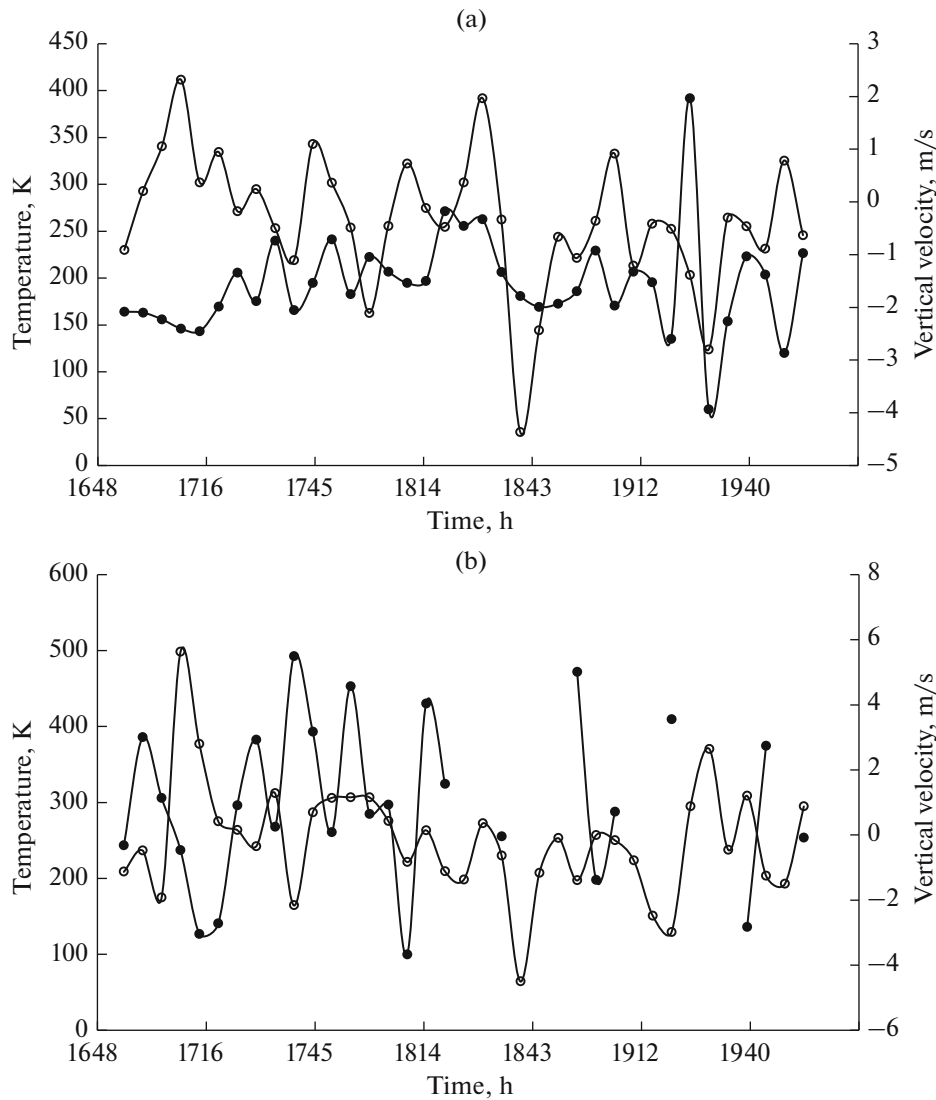
Fig. 10. Temporal dependence of the temperature (points) and velocity of vertical motion of the medium (circles) at an altitude of 105 km (a) and 112 km (b) based on observations on August, 9, 2017.

while they are in the "opposite phase" in all other cases. In this case, the vertical velocity, as a rule, constantly changes its direction. The event is somewhat different in the altitude range of 90−100 km. In this altitude range, the changes in temperature and velocity are in the "opposite phase," except for the 1130 session. There is no doubt that such changes in the altitude profiles of T and V, which go beyond the measurement errors, are an objective reflection of the processes occurring at the altitudes of the mesosphere and lower thermosphere. However, it is not yet clear which atmospheric processes cause such features of the altitude profiles of temperature and velocity: atmospheric waves, heat transfer by thermal diffusion, or heating due to turbulence dissipation. In our opinion, it may be important to take into account the fast turbulence of the neutral component. Rapid variations

were noted even in the first experiments on the ionosphere with the API method and digital recording of the amplitude and phase of the scattered signal with a time resolution of 15 s. They naturally manifest themselves in the characteristics of the ionosphere and the neutral atmosphere, which are determined based on these records. Belikovich et al. (1999) and Bakhmetieva et al. (2020) gave examples of the dependence of the turbulent velocity on time, as measured with a time resolution of 15 s and averaged over each minute, in which fast 15-s and 1-min variations are clearly seen. In our opinion, the fast turbulence is caused by the scattering of probe radio waves by natural D-region inhomogeneities (called partial reflections), which, as a rule, occupy an altitude range of 60−90 km. They also contribute to the value of the turbulent velocity V_t.

Such profiles of temperature and velocity were discussed earlier (Bakhmetyeva et al., 2010b, 2017; Tolmacheva et al., 2013; Tolmacheva et al., 2013). The altitude profiles of temperature $T(h)$ with a negative altitude gradient and the subsequent development of the temperature and density perturbations of the neutral component are presented in the literature (Tolmacheva et al., 2013; Bakhmetieva et al., 2017b; Tolmacheva et al., 2019). Tolmacheva et al. (2013) showed that the instability of the medium plays an important role in temperature variations. In the approximation of a linear altitude dependence of temperature, the observing condition $dT/dh < -(10-12\ \text{K/km})$ is a sufficient condition for the development of instability. The excitation of IGWs of different periods and associated instabilities should lead to turbulization of the medium, which manifests itself in the parameters of the signal scattered by inhomogeneities. The argument in favor of an increase in the level of medium turbulization is the existence of the turbulent velocities given above, which are relatively large (up to 5–10 m/s). Tolmacheva et al. (2013) concluded based on an analysis of a large volume of altitudinal-temporal dependences of temperature and velocity that convective instabilities can be observed when IGWs propagate above 100 km; this ensures energy transfer from the turbulent region to the lower thermosphere.

Figure 9 shows the temporal dependence of the velocity of vertical motion at an altitude of 100 km (a) and 105 km (b) during observations on October 25, 2018. The remaining altitudes are not shown to simplify the figure. Each point on the graph was obtained via averaging of the velocity values over 5 min. The dashed curve was formed via running averaging over an interval of 40 min (eight points) in order to smooth out fluctuations of smaller periods. An irregular change in the direction of the velocity in time with quasiperiodic variations is noted. Scatter of the velocity values during adjacent 5-min measurements was found at some time moments and reached 5–7 m/s, while averaging neutralizes a more significant scatter of instantaneous values (in one dimension). The period of undulating variations increases with altitude, which is typical for IGWs (Gossard and Hook, 1978; Fritts and Alexander, 2003).

Figure 10 shows the temporal dependence of the temperature (dots) and velocity of vertical motion of the medium (circles) at an altitude of 105 km (Fig. 1a) and 112 km (Fig. 1b) based on the observations on August 9, 2017. As for the altitude profiles, both the correlation and anticorrelation of time variations of these values are found at both altitudes. A limited number of temperatures were measured at an altitude of 112 km due to violation of the diffusion approximation of the altitude dependence of the relaxation time. At this altitude, which is anomalously large in our opinion, the values of T were also measured. There is no doubt about the influence of the propagation of atmospheric waves on the temperature and velocity of

the medium propagation. The periods of waves and their contribution to the changes in temperature and vertical velocity, as well as their manifestation in variations in the velocities of turbulent motions and variations in the turbopause level, correspond to the parameters of IGWs (Hines, 1975; Karimov, 1983; Brunelli and Namgaladze, 1988; Grigoriev, 1999; Fritts and Alexander, 2003; Somsikov, 2011; Karpov et al., 2016; Borchevkina and Karpov, 2018).

7. CONCLUSIONS

The paper presents new results from the study of atmospheric dynamics, which supplement the previous information on the turbulence and dynamics of the lower ionosphere. The velocity of the vertical regular motion of plasma, the turbopause level, the velocity of turbulent motions, and the temperature of the neutral component were determined from measurements of the amplitude and phase of the signal scattered by APIs based on an analysis of their altitudinal-temporal dependences. The high temporal resolution of the method applied here made it possible to study fast temporal variations in the parameters. It follows from the results presented in the work that the velocities of turbulent motions, which amount to several m/s, are comparable in magnitude with the velocity of the vertical regular motion of the plasma and the neutral component. The turbopause level in the altitude interval 88–110 km is subjected to both fast and slow changes. The wave character of the turbopause level has been noted. This result is important for the dynamics of the lower ionosphere from the point of view of the study of atmospheric wave processes. Note that turbulent and regular motions are easily distinguished by the measured phase of the scattered signal, which has a "chaotic" character of change in the case of turbulence. The altitudinal-temporal variations of the parameters of the neutral component have convincingly demonstrated the significant influence of wave processes on them. Changes in parameters over time occur with a frequency characteristic of IGWs.

REFERENCES

Andreeva, L.A., Klyuev, O.F., Portnyagin, Yu.I., and Khanan'yan, A.A., *Issledovanie protsessov v verkhnei at-*

mosfere metodom iskusstvennykh oblakov (Study of Upper Atmospheric Processes by the Artificial Cloud Method), Leningrad: Gidrometeoizdat, 1991.

Axford, W.I. and Cunnold, D.M., The wind shear theory of temperate zone sporadic E, *Radio Sci.*, 1966, vol. 1, no. 2, pp. 191−197.

Bakhmet'eva, N.V., Belikovich, V.V., and Korotina, G.S., Determination of Turbulent Velocities with the Use of Artificial Periodic Inhomogeneities, *Geomagn. Aeron. (Engl. Transl.)*, 1996a, vol. 36, no. 5, pp. 724−726.

Bakhmet'eva, N.V., Belikovich, V.V., Benediktov, E.A., Bubukina, V.N., Goncharov, N.P., and Ignat'ev, Yu.A., Seasonal and diurnal variations of vertical motion velocities within mesosphere and lower thermosphere near Nizhnii Novgorod, *Geomagn. Aeron. (Engl. Transl.)*, 1996b, vol. 36, no. 5, pp. 675−681.

Bakhmet'eva, N.V., Belikovich, V.V., Grigor'ev, G.I., and Tolmacheva, A.V., Effect of acoustic gravity waves on variations in the lower-ionosphere parameters as observed using artificial periodic inhomogeneities, *Radiophys. Quantum Electron.*, 2002, vol. 45, no. 3, pp. 233−242.

Bakhmet'eva, N.V., Belikovich, V.V., Kagan, L.M., and Ponyatov, A.A., Sunset−sunrise characteristics of sporadic layers of ionization in the lower ionosphere observed by the method of resonance scattering of radio waves from artificial periodic inhomogeneities of the ionospheric plasma, *Radiophys. Quantum Electron.*, 2005, vol. 48, no. 1, pp. 14−28.

Bakhmet'eva, N.V., Belikovich, V.V., Bubukina, V.N., Vyakhirev, V.D., Kalinina, E.E., Komrakov, G.P., and Tolmacheva, A.V., Results of determining the electron number density in the ionospheric *E* region from relaxation times of artificial periodic irregularities of different scales, *Radiophys. Quantum Electron.*, 2008, vol. 51, no. 6, pp. 431−437.

Bakhmet'eva, N.V., Belikovich, V.V., Egerev, M.N., and Tolmacheva, A.V. Artificial periodic irregularities, wave phenomena in the lower ionosphere and the sporadic *E*-layer, *Radiophys. Quantum Electron.*, 2010a, vol. 53, no. 9, pp. 77−90.

Bakhmet'eva, N.V., Grigor'ev, G.I., and Tolmacheva, A.V., Artificial periodic irregularities, hydrodynamic instabilities, and dynamic processes in the mesosphere−lower thermosphere, *Radiophys. Quantum Electron.*, 2010b, vol. 53, no. 11, pp. 623−637.

Bakhmetieva, N.V., Bubukina, V.N., Vyakhirev, V.D., Grigoriev, G.I., Kalinina, E.A., and Tolmacheva, A.V., The results of comparison of vertical motion velocity and neutral atmosphere temperature at the lower thermosphere heights, *Proc. 5th Int. Conf. "Atmosphere, Ionosphere, Safety,"* Kaliningrad, 2016a, pp. 197−202.

Bakhmetieva, N.V., Grach, S.M., Sergeev, E.N., Shindin, A.V., Milikh, G.M., Siefring, C.L., Bernhardt, P.A., and McCarrick, M., Artificial periodic irregularities in the high-latitude ionosphere excited by the HAARP facility, *Radio Sci.*, 2016b, vol. 51, no. 7, pp. 999−1009.

Bakhmet'eva, N.V., Bubukina, V.N., Vyakhirev, V.D., Kalinina, E.E., and Komrakov, G.P., Response of the lower ionosphere to the partial solar eclipses of August 1, 2008 and March 20, 2015 based on observations of radio-wave scattering by the ionospheric plasma irregularities, *Radiophys. Quantum Electron.*, 2016c, vol. 59, no. 10, pp. 782−793.

Bakhmet'eva, N.V., Vyakhirev, V.D., Kalinina, E.E., and Komrakov, G.P., Earth's lower ionosphere during partial solar eclipses according to observations near Nizhny Novgorod, *Geomagn. Aeron. (Engl. Transl.)*, 2017a, vol. 57, no. 1, pp. 58−71.

Bakhmetieva, N.V., Bubukina, V.N., Vyakhirev, V.D., Grigoriev, G.I., Kalinina, E.E., and Tolmacheva, A.V., The results of comparison of vertical motion velocity and neutral atmosphere temperature at the lower thermosphere heights, *Russ. J. Phys. Chem. B.*, 2017b, vol. 11, no. 6, pp. 1017−1023.

Bakhmet'eva, N.V., Vyakhirev, V.D., Kalinina, E.E., and Komrakov, G.P., Earth's lower ionosphere during partial solar eclipses according to observations near Nizhny Novgorod, *Geomagn. Aeron. (Engl. Transl.)*, 2017c, vol. 57, no. 1, pp. 58−71.

Bakhmet'eva, N.V., Grigoriev, G.I., Tolmacheva, A.V., and Kalinina, E.E., Atmospheric turbulence and internal gravity waves examined by the method of artificial periodic irregularities, *Russ. J. Phys. Chem. B.*, 2018, vol. 12, no. 3, pp. 510−521.

Bakhmetieva, N.V., Grigoriev, G.I., Tolmacheva, A.V., and Zhemyakov, I.N., Investigations of atmospheric waves in the Earth lower ionosphere by means of the method of the creation of the artificial periodic irregularities of the ionospheric plasma, *Atmosphere*, 2019, vol. 10, no. 8, id 450.
https://doi.org/10.3390/atmos10080450

Bakhmetieva, N.V., Vyakhirev, V.D., Grigoriev, G.I., Egerev, M.N., Kalinina, E.E., Tolmacheva, A.V., Zhemyakov, I.N., Vinogradov, G.R., and Yusupov, K.M., Dynamics of the mesosphere and lower thermosphere based on results of observations on the SURA facility, *Geomagn. Aeron. (Engl. Transl.)*, 2020a, vol. 60, no. 1, pp. 96−111.

Bakhmetieva, N.V., Kulikov, Yu.Yu., and Zhemyakov, I.N., Mesosphere ozone and the lower ionosphere under plasma disturbance by powerful high-frequency radio emission, *Atmosphere*, 2020b, vol. 11, no. 11, id 1154.
https://doi.org/10.3390/atmos11111154

Belikovich, V.V. and Benediktov, E.A., Influence of atmospheric turbulence on the relaxation of a signal scattered by artificial periodic inhomogeneities, *Geomagn. Aeron.*, 1995, vol. 35, no. 2, pp. 91−99.

Belikovich, V.V., Benediktov, E.A., Tolmacheva, A.V., and Bakhmet'eva, N.V., *Issledovanie ionosfery s pomoshch'yu iskusstvennykh periodicheskikh neodnorodnostei* (Study of the Ionosphere using Artificial Periodic Inhomogeneities), N. Novgorod: IPF RAN, 1999.

Belikovich, V.V., Benediktov, E.A., Tolmacheva, A.V., and Bakhmet'eva, N.V., *Ionospheric Research by Means of Artificial Periodic Irregularities*, Katlenburg-Lindau, Germany: Copernicus, 2002.

Belikovich, V.V., Bakhmet'eva, N.V., Kalinina, E.E., and Tolmacheva, A.V., A new method for determination of the electron number density in the *E* region of the ionosphere from relaxation times of artificial periodic inhomogeneities, *Radiophys. Quantum Electron.*, 2006, vol. 49, no. 9, pp. 699−674.

Borchevkina, O.P. and Karpov, I.V., Observations of variations in total electron content in the solar terminator region in the ionosphere, *Sovrem. Probl. Distantsionnogo*

Zondirovaniya Zemli Kosmosa, 2018, vol. 15, no. 1, pp. 299−305.

Bryunelli, B.E. and Namgaladze, A.A., *Fizika ionosfery* (Physics of the Ionosphere), Moscow: Nauka, 1988.

Danilov, A.D., Kalgin, U.A., and Pokhunkov, A.A., Variation of the turbopause level in the polar regions, *Space Res.*, 1979, vol. 19, no. 83, pp. 173−176.

Fritts, D.C. and Alexander, M.J., Gravity waves dynamics and effects in the middle atmosphere, *Rev. Geophys.*, 2003, vol. 41, no. 1.

Galedin, I.F., Neelov, I.O., and Pakhomov, S.V., Estimates for turbulent diffusivity in the mesosphere obtained by the radiolocation method, *Tr. Tsentr. Astrofiz. Obs.*, 1981, no. 144, pp. 22−27.

Gershman, B.N., *Dinamika ionosfernoi plazmy* (Dynamics of Atmospheric Plasma), Moscow: Nauka, 1974.

Gershman, B.N., Ignat'ev, Yu.A., and Kamenetskaya, G.Kh., *Mekhanizmy obrazovaniya sporadicheskogo sloya E_s na raznykh shirotakh* (Mechanisms of the Formation of the Sporadic Layer E_s at Various Latitudes), Moscow: Nauka, 1976.

Gossard, E.E. and Hook, W.H., *Waves in the Atmosphere*, Amsterdam: Elsevier, 1975; Moscow: Mir, 1978.

Grigor'ev, G.I., Acoustic−gravity waves in the Earth's atmosphere (review), *Radiophys. Quantum Electron.*, 1999, vol. 42, no. 1, pp. 1−21.

Haines, K.O., Atmospheric gravity waves, in *Thermospheric Circulation*, Webb, W.L., Ed., Cambridge: MIT, 1972; Moscow: Mir, 1975, pp. 85−99.

Hall, C.M., Holmen, S.E., Meek, C.E., Manson, A.H., and Nozawa, S., Change in turbopause altitude at 52 and 79° N, *Atmos. Chem. Phys.*, 2016, vol. 16, no. 4, pp. 2299−2308.

Hocking, W.K., On the extraction of atmospheric turbulence parameters from radar backscatter Doppler spectra-I: Theory, *J. Atmos. Terr. Phys.*, 1983a, vol. 45, nos. 2−3, pp. 89−102.

Hocking, W.K., Mesospheric turbulence intensities measured with a HF radar at 35°S−II, *J. Atmos. Terr. Phys.*, 1983b, vol. 45, nos. 2−3, pp. 103−114.

Hocking, W.K., Dynamical coupling processes between the middle atmosphere and lower ionosphere, *J. Atmos. Terr. Phys.*, 1996, vol. 58, no. 6, pp. 735−752.

Hocking, W.K. and Roettger, J., The structure of turbulence in the middle and lower atmosphere seen by and deduced from MF, HF and VHF radar, with special emphasis on small-scale features and anisotropy, *Ann. Geophys.*, 2001, vol. 19, no. 8, pp. 933−944.

Holdsworth, D.A., Vincent, R.A., and Reid, I.M., Mesospheric turbulent velocity estimation using the Buckland Park MF radar, *Ann. Geophys.*, 2001, vol. 19, no. 8, pp. 1007−1017.

Izmerenie vetra na vysotakh 90−100 km nazemnymi metodami (Measurements at Altitudes of 90−100 km by Ground-Based Methods), Portnyagin, Yu.I. and Sprenger, K., Eds., Leningrad: Gidrometeoizdat, 1978.

Kagan, L.M., Bakhmet'eva, N.V., Belikovich, V.V., and Tolmacheva, A.V., Structure and dynamics of sporadic layers of ionization in the ionospheric e region, *Radio Sci.*, 2002, vol. 37, no. 6, pp. 1106−1123.

Kalgin, Yu.A. and Danilov, A.D., Determination of eddy diffusivity parameters in the mesosphere and lower thermosphere, *Geomagn. Aeron.*, 1993, vol. 33, no. 6, pp. 119−125.

Karimov, K.A., *Vnutrennie gravitatsionnye volny v verkhnei atmosfere* (Internal Gravity Waves in the Upper Atmosphere), Frunze: Ilim, 1983.

Karpov, I.V. and Kshevetskii, S.P., Formation of large-scale disturbances in the upper atmosphere caused by acoustic gravity wave sources on the Earth's surface, *Geomagn. Aeron. (Engl. Transl.)*, 2014, vol. 54, no. 4, pp. 513−522.

Karpov, I.V., Kshevetskii, S.P., Borchevkina, O.P., Radievskii, A.V., and Karpov, A.I., Disturbances of the upper atmosphere and ionosphere caused by acoustic-gravity wave sources in the lower atmosphere, *Russ. J. Phys. Chem. B*, 2016, vol. 35, no. 1, pp. 127−132.

Khanan'yan, A.A., On atmospheric stability at heights from 80 to 130 km, in *Tr. Inst. Eksp. Meteorol. Fiz. Verkhn. Atmos.*, 1982, no. 11, pp. 75−77.

Khanan'yan, A.A., The vertical structure of wind and turbulence in the lower thermosphere of midlatitudes, *Issledovanie dinamicheskikh protsessov v verkhnei atmosfere* (Study of Dynamical Processes in the Upper Atmosphere), Lysenko, I.A., Ed., Moscow: Gidrometeoizdat, 1985, pp. 59−63.

Kirkwood, S., Seasonal and tidal variations of neutral temperatures and densities in the high latitude lower thermosphere measured by EISCAT, *J. Atmos. Terr. Phys.*, 1986, vol. 48, pp. 817−826.

Kokin, G.A. and Pakhomov, S.V., The turbulent regime of region D in the winter of 1983−1984, *Geomagn. Aeron.*, 1986, vol. 26, no. 5, pp. 714−717.

Lehmacher, G.A., Scott, T.D., Larsen, M.F., Bilen, S.G., Croskey, C.L., Mitchell, J.D., Rapp, M., Lübken, F.-J., and Collins, R.L., The Turbopause experiment: Atmospheric stability and turbulent structure spanning the turbopause altitude, *Ann. Geophys.*, 2011, vol. 29, no. 12, pp. 2327−2339.

Mathews, J.D., Sporadic E: Current views and recent progress, *J. Atmos. Sol.-Terr. Phys.*, 1998, vol. 60, no. 4, pp. 413−435.

Medvedeva, I.V. and Ratovsky, K.G., Comparative analysis of atmospheric and ionospheric variability by measurements of temperature in the mesopause region and peak electron density $NmF2$, *Geomagn. Aeron. (Engl. Transl.)*, 2017, vol. 57, no. 2, pp. 217−228.

Offermann, D., Jarisch, M., Oberheide, J., Gusev, O., Wohltmann, I., Russel, III J.M., and Mlynczak, M.G., Global wave activity from upper stratosphere to lower thermosphere: A new turbopause concept, *J. Atmos. Sol.−Terr. Phys.*, 2006, vol. 68, no. 15, pp. 1709−1729.

Perminov, V.I., Semenov, A.I., Medvedeva, I.V., and Pertsev, N.N., Temperature variations in the mesopause region according to the hydroxyl-emission observations at midlatitudes, *Geomagn. Aeron. (Engl. Transl.)*, 2014, vol. 54, no. 2, pp. 230−239.

Pokhunkov, A.A., Rybin, V.V., and Tulinov, G.F., Atomic oxygen trend in the midlatitude and equatorial thermosphere, *Geomagn. Aeron. (Engl. Transl.)*, 2003, vol. 43, no. 5, pp. 641−646.

Schlegel, K., Brekke, A., and Haug, A., Some characteristics of the quiet polar D-region and mesosphere obtained with the partial reflection method, *J. Atmos. Terr. Phys.*, 1977, vol. 40, no. 2, pp. 205−213.

Sherstyukov, O.N. and Stenin, Yu.M., Impact of turbulent irregularities on the semi-transparency of the E_s layer, *Geomagn. Aeron. (Engl. Transl.)*, 2002, vol. 42, no. 1, pp. 96−100.

Somsikov, V.M., Solar terminator and dynamic phenomena in the atmosphere: A review, *Geomagn. Aeron. (Engl. Transl.)*, 2011, vol. 51, no. 6, pp. 707−719.

Teptin, G.M. and Stenin, Yu.M., On the spectrum of electron concentration inhomogeneities in the lower ionosphere, *Dokl. Akad. Nauk SSSR*, 1977, vol. 233, no. 1, pp. 85−88.

Tolmacheva, A.V., Grigoriev, G.I., and Bakhmetieva, N.V., The variations of the atmospheric parameters on measurements using the artificial periodic irregularities of plasma, *Russ. J. Phys. Chem. B*, 2013, vol. 7, no. 5, pp. 663−669.

Tolmacheva, A.V., Bakhmetieva, N.V., Grigoriev, G.I., and Kalinina, E.E., The main results of the long-term measurements of the neutral atmosphere parameters by the artificial periodic 63 irregularities techniques, *Adv. Space Res.*, 2015, vol. 56, no. 6, pp. 1185−1193.

Tolmacheva, A.V., Bakhmetieva, N.V., Grigoriev, G.I., and Egerev, M.N., Turbopause range measured by the method of the artificial periodic irregularities, *Adv. Space Res.*, 2019, vol. 64, no. 10, pp. 1968−1974.

Vlasov, M.N. and Kelley, M.C., Specific features of eddy turbulence in the turbopause region, *Ann. Geophys.*, 2014, vol. 32, no. 4, pp. 431−442.

Vlasov, M.N. and Kelley, M.C., Eddy diffusion coefficients and their upper limits based on application of the similarity theory, *Ann. Geophys.*, 2015, vol. 33, no. 7, pp. 857−864.

Whitehead, J.D., Recent work on mid-latitude and equatorial sporadic-E, *J. Atmos. Terr. Phys.*, 1989, vol. 51, no. 5, pp. 401−424.

Translated by E. Morozov